Mathematical Modelling and Experimental Study of an Enhanced Double-Slope Glass Solar Still

Mohammed Alswat

Abstract — **Solar desalination is considered an important technology for solving the water shortage problem. In this research, a mathematical modeling and experimental study of an enhanced double-slope glass solar still were developed and evaluated based on a comparison with the conventional one. The two solar still were designed and fabricated at the Faculty of Engineering, University of Tabuk, and compared in the same operating climate conditions. The solar radiation model was developed, tested, and used with the solar still mathematical modeling to predict water productivity and daily efficiency. Copper T shape pieces were used in the solar still basin to increase the free water surface area inside the still at a water depth of 3 cm. The results indicated that the average measured and calculated values of accumulated productivity for conventional solar still were 3.01 and 3.32 L/m^2.day respectively with a deviation of 9.3%. The corresponding average values for the enhanced solar still were 7.03 and 8.16 L/m^2.day respectively. In addition, it can be noticed that the maximum measured daily thermal efficiency was about 56.4% and 25.31% for enhanced and conventional solar still respectively. Also, the cost evaluation was performed, and the results concluded that the enhanced double-slope glass solar still with cost per liter was about 0.0024 $/L/m^2. The modeling and experimental results were compared based on the statistical evaluation methods and it is clear that the proposed mathematical model gives a good prediction of solar radiation and performance for the enhanced double-slope glass solar still.**

Keywords — **Mathematical Performance, Solar Still, Solar Radiation, Still Efficiency.**

I. Introduction

The potable water shortage has become an important factor restricting the development of the world, especially in the economic. In coastal regions with high population density, the shortage of water resources will become a matter of economic and social development and one of the major issues that facing the future generations. Desalination is to increase water resources from the source, and it is a strategic choice to solve the lack of potable water resources in the world [1]. Many researchers are working to develop desalination technologies, different methods are designed based on different principles, such as phase-change processes and membrane processes. The main disadvantage of using these techniques is the energy usage and the energy consumption [2]. Using solar energy in desalination processes is regarded as one of the most cost-effective ways to obtain drinking water. One of the most popular techniques in desalination is the using of solar still in the desalination process. Solar still productivity is considered low compared with the different types [3].

El-Agouz [4] evaluated the stepped solar still performance using water circulation with the conventional one. From the results, it can be noticed that the still productivity is higher than the conventional solar still by 43% by using seawater and by 48% by using salt water with a black absorber. The productivity increased by 53% and 47% for sea and salty water, respectively. The performance of solar still by using glass as the basin material was performed by Elango and Murugavel [5]. They carried out their study by changing the water depths from 1 to 5 cm with insulated and uninsulated conditions. The findings showed that the production of a single basin is more than the double basin during the heating period. Kabeel *et al.* [6] evaluated the performance of a modified solar still using a stream of hot air injection and phase change material in a single slope solar still. They concluded that the water productivity of the modified solar still was about 108% more than the conventional one. Altarawneh *et al.* [7] optimized an experimental and numerical analysis for the single, double slope, and pyramidal-shaped solar stills performance. They concluded that the single-slope solar still improved productivity by 28%. Hansen and Murugavel [8] presented an experimental study for the enhancement of solar still using a new absorber. Their obtained results indicated that the daily productivity of the combined still with finned absorber was about 74.3%. Rahbar *et al.* [9] evaluated the performance of two different solar stills of dissimilar geometries namely tubular and triangular. They concluded that the efficiency of the tubular and triangular was about 41% and 35% respectively and the water productivity for one week was about 1.6 l/m^2 and 1.34 l/m^2 respectively. Nazari *et al.* [10] performed theoretical and experimental study on single-slope solar still using nanofluid and thermoelectric condensing tube. They concluded that the yield and energy efficiencies using thermoelectric condensing tube increased by 38.5% and 38.9% respectively. In addition using nanofluid increased the productivity, energy by 82.4% and 81.5% respectively. Dumk *et al.* [11] evaluated the performance of a single slope solar still with sand-filled cotton to increase the water surface area. They concluded that water productivity increased by 28.56% and 30.99% in for basin water of 30 and 40 kg respectively. Gnanaraj and Velmurugan [12] presented experimental research for the double slope solar still. Three modifications were used; finned corrugated basin, still with black granite and

Submitted on October 02, 2022.
Published on November 01, 2022.

M. Alswat, Department of Mechanical Engineering, University of Tabuk, Saudi Arabia.
(e-mail: malswat@ut.edu.sa)

still with wick with internal and external modifications. The results concluded that the solar still productivity by using external and internal modifications was about 5130 ml/m^2 per day.

Kabeel and Abdelgaied [13] used absorbers with high thermal conductivity to enhance the pyramid-shaped solar still performance. They used graphite in the still basin and compared the results with the same still without modifications. The obtained results showed that the daily productivity ranged from 105.9 to 107.7%, while the efficiency ranged from 97.2 to 98.9% compared with the traditional pyramid. Abdullah *et al.* [14] improved the solar still performance by using phase change material and reflectors. Their results indicated that the maximum obtained efficiency was about 51.5%, compared to 35% percent for the conventional one. Kabeel *et al.* [15] performed experimental research to improve the performance of pyramid-shaped solar stills by using phase change materials and hollow circular fins. Their results indicated that using the hollow fins improved the daily productivity by 43 % and using the PCM with fins increased the production by 101.5 %. Sharshir *et al.* [16] enhanced the performance of the solar still by using cotton fabric, floating coal and carbon black nanoparticles. The results indicated that the highest enhancements in productivity was about 59.33% compared to the conventional one. Saravanan *et al.* [17] designed and fabricated a single basin double slope solar still using kanchey marbles as an energy storage material. The obtained results concluded that using kanchey marbles enhanced the still performance by 16.32%. Agrawal and Singh [18] evaluated the performance of the solar still using binary eutectic PCM and steel wool fibre. The obtained results showed that the total productivity reached to 3.40 kg/m^2. Parsa *et al.* [19] used different nanoparticles to increase the still performance. The findings showed that the thermal efficiency improved by 38.2% compared to the conventional system. Jobrane *et al.* [20] performed numerical and experimental three different ideas to improve the still efficiency. Their results concluded that the water productivity was about 4.03 L.m^2 per day. In addition the numerical results were validated with the experimental, and the efficiency of the solar still was enhanced by 32%. Abdelgaied *et al.* [21] designed and fabricated two solar distillers and used interior mirrors, nanoparticles-coated absorber surface and PCM in Tanta, Egypt. Their results showed that the water productivity reached 9.79 L/m^2 per day compared to 4.15 L/m^2/day achieve by the reference solar still. The obtained average daily thermal efficiency of the reference still reached to 33.3%, and the modified stepped solar still was about 78.8%. Ahmed *et al.* [22] gave a detailed analysis on solar stills performance and the productivity enhancement methods for different types of solar stills. In their study, they discussed the factors that affecting the still performance which include the design parameters, the climatic conditions and the operations methods.

In this study mathematical model of solar radiation was performed to calculate and predict the solar radiation over any country over the world. In addition an enhanced double slope glass solar still was fabricated and designed at faculty of Engineering, University of Tabuk. Copper T shape pieces are used in the still basin to increase the free water surface area with hot air inside the still to increase water productivity. Also, a mathematical model for the still performance and productivity was built and used with the solar radiation model to calculate and predict the solar still productivity. Finally the present work was compared with the previous publications and the cost evaluation was studied based on the calculation parameters.

II. Materials and Methods

In this section, the experimental setup has been described in detail. Measured parameters and measuring instruments are also presented. The experimental procedure is explained, and the error analysis was estimated. The experimental work was designed and fabricated at the Faculty of Engineering, University of Tabuk. The experimental work consists of an enhanced double slope glass solar still, conventional type one, water tank and the connecting pipes. The solar stills were constructed from materials that are readily available in the local area. The experimental setup layout is shown in Fig. 1. The two solar stills were connected with data acquisition to record the temperatures using k-type thermocouples. The measured temperatures are absorber, water, space, and glass temperatures. The ambient temperature, intensity of solar radiation and wind velocity are also measured.

A. The Enhanced Double Slope Glass Solar Still

Fig. 2 shows a schematic diagram of the enhanced double slope glass solar still with the k-type thermocouples positions. The enhanced double slope glass solar still consists of a galvanized iron basin and a glass transparency cover (5 mm thick). Galvanized iron sheet with 0.7 mm thick was used due to its good resistance to corrosion, low weight and easy formation. The side wall and the base plate absorber of the still are black painted to increase the solar absorptivity of the falling solar radiation inside the still. Plastic collection duct is used to collect the water productivity. The water condensate trickles into the collection duct under gravity action. Silicon rubber material is used to prevent the leakage from any point gap in the still. Three main holes are made in the still; the first hole is connected with PVC pipe used to feed the saline water into the still. The second one is used to collect the distilled water in a bottle. The third hole is used as a drain. A glass U-tube manometer was used to adjust the water level at the still and calibrated for water levels from 1 to 10 cm. The solar still is mounted in a box with four legs to decrease the heat loss to the ground. The overall dimensions of the still are shown in Fig. 2 and basin area is equal to 1 m^2, height is equal to 33 cm.

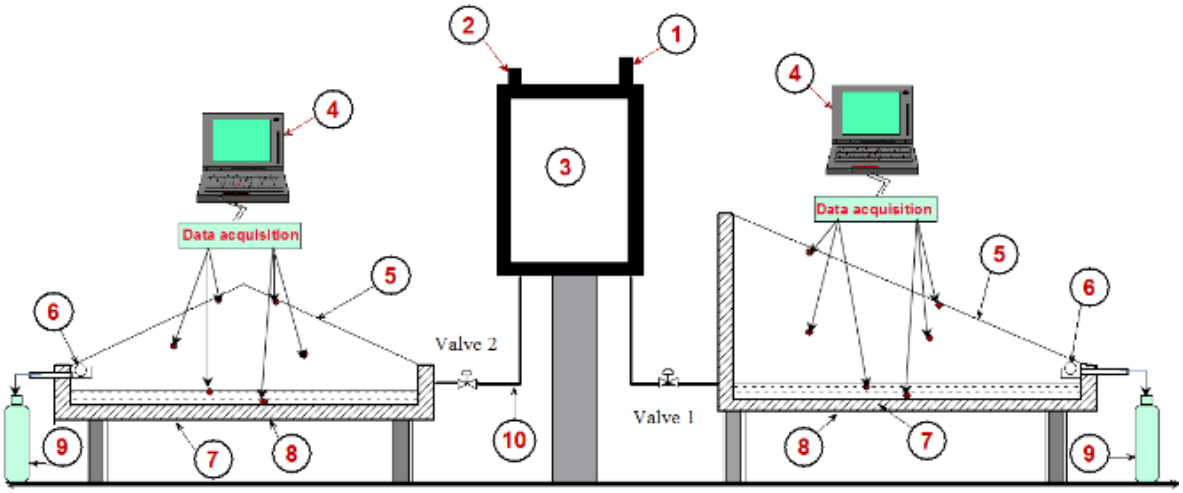

1- Water inlet
2- Air vent
3- The feed water tank
4- Data acquisition
5-Glass cover
6- Distillate collection
7- Insulation
8- Frame
9- Bottle
10- PVC pipes

Fig. 1. The experimental setup layout.

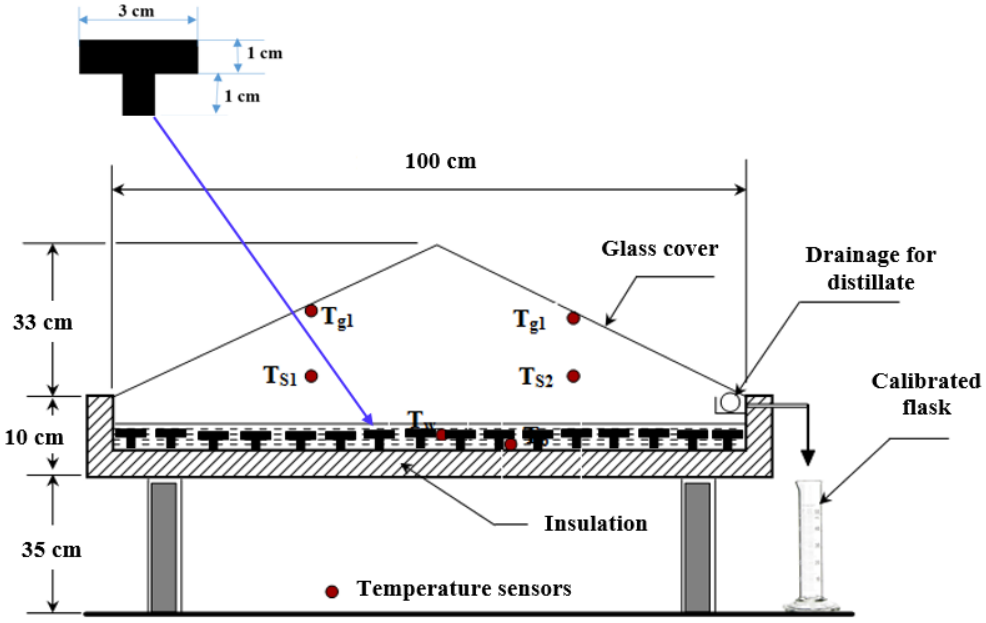

Fig. 2. The enhanced double slope glass solar still schematic diagram.

In order to increase the free water surface area with hot air inside the still, copper T shape pieces are used in the enhanced solar still basin. The copper T shape pieces also can reduce the surface tension between water molecules; therefore the water molecules evaporate in a high rate. The molecules leave the free water surface of the easiest and quickest way bound for the glass cover. In this experiment, 20 copper T shape pieces (dimensions L × W × H of 100 × 3 × 2 cm) were used in the enhanced solar still in each experiment. The base dimensions of the copper T shape pieces are fixed at the still basin and painted black to increase the absorber solar energy. Using copper T shape pieces lead to an increase the absorber area and more water is exposed to solar radiation, decreasing the preheating period of the water and increasing the productivity of the still. The above experiment was performed for nine days to choose and compare the results in closed days with similar weather characteristics. The received radiation by the copper T shape pieces are divided into two parts. The first one is used to heat the water top layer and increases the water temperature while the second part is stored in the water bottom and released during low solar intensity periods. The copper T shape pieces were placed in the still basin so that, the height of the water above it always depends on the water depth in the still basin as shown in Fig. 2. In order to compare the results of the enhanced solar still, a conventional solar still (a single basin) has been designed and fabricated as a reference with the same materials and dimensions. The conventional solar still with the k-type thermocouples positions is shown in Fig. 3. The basin is covered with a single sloped transparent glass sheet 5 mm thick inclined at 31° to horizontal.

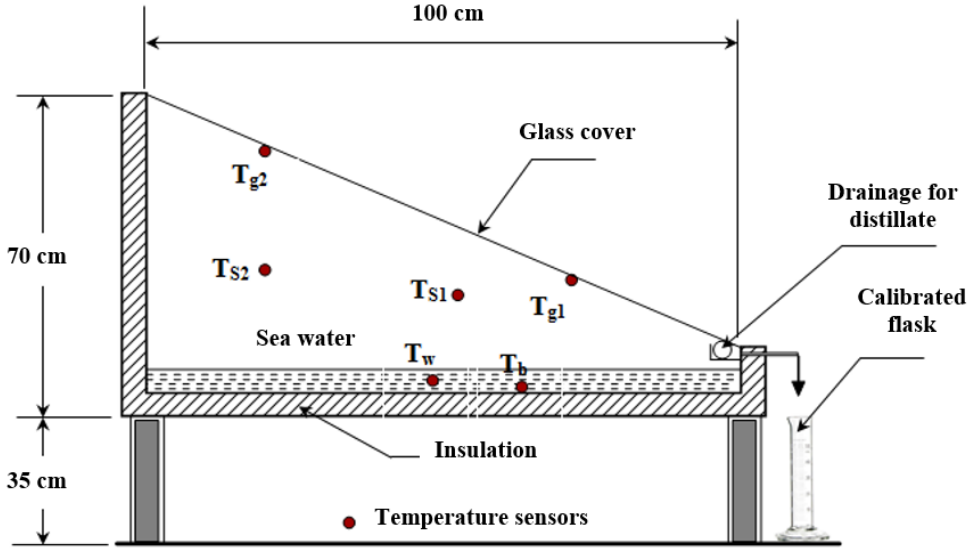

Fig. 3. The conventional solar still schematic diagram.

Good silicon rubber sealant is used to prevent the escape of water vapor to the ambient. Three holes are made for drainage, distilled water output, and for feeding saline water into the still. The output from the still is collected through a trough into the bottle, fixed near the still basin. The conventional solar still basin has an area of 1 m^2 (100 cm × 100 cm). The high-side wall of the still is 70 cm and the low-side wall height is 10 cm. The general properties of the solar stills are listed in Table I and the two solar stills are operating at the same climate conditions. The feed water is injected to the still continuously during the operation from the water storage tank. A feed water tank of 0.50 × 0.50 × 0.80 m^3 is used to feed water the solar stills as shown in Fig. 1.

TABLE I: GENERAL PROPERTIES OF THE SOLAR STILLS

No.	General properties	Value
1	Solar still area	1 m^2
2	Cover material	glass
3	Insulation material	foam
4	Thickness of insulation	0.05 m
5	Thickness of glass	0.05 m
6	Height of water basin	0.10 m
7	Glass angle inclination	31°

B. Measurements and Instruments

This part presents the instruments which are used to measure the different parameters like temperatures inside the solar stills, global solar radiation, wind velocity and ambient conditions. Conductivity and the total dissolved solids were also measured at the beginning and end of each experiment for the used water. Fig. 4 shows the photograph of the measurements and instruments in the experiment setup. Seven k-type thermocouples were used in different positions to measure the temperatures inside the solar still as illustrated in Figs. 2 and 3. The air temperature sensors were fixed 20 cm above the still basin in east and west directions. Also, the glass cover temperature sensors were fixed in glass cover inner surface at the directions of east and west. These sensors have a data logger with four ports for collecting the measured data during the experimental days and the measured data is displayed on the screen as shown in Fig. 4a.

Solar radiation is the basic parameter in desalination processes. In this work, solar power meter was used to measure the global solar radiation during the experimental days. The apparatus sensor is connected with a digital output screen to record the measured output values. The apparatus is designed to measure the global solar radiation in watts per meter square. Fig. 4b shows a photograph of the solar power meter with an output screen. In this work, salty and freshwater were used during each experiment. The salty and freshwater conductivity/total dissolved solids (TDS) were measured with CyberScan CON 11 as shown in Fig. 4c. This device is easy to use without troubleshooting and automatically selectable between different units of conductivity and TDS. At the beginning and end of the working day, the fresh and salty feed water conductivity / TDS were measured. Also, these measurements were done for the output water productivity. The wind velocity is an important parameter that affects the solar still performance. During each day of experiments, the wind velocity was measured every 60 minutes time interval. Digital advanced anemometer type Xplorer-4 is used to measure the wind velocity as shown in Fig. 4d. The device is high precision and fitted with an impeller which allows it to carry out measurements in the open air. The apparatus measuring range is from 0 to 42 m/s. The device records the instant wind velocity, the maximum wind velocity, ambient temperature, altitude, and atmospheric pressure. The average values of wind velocity were calculated during the experimental days. The hourly condensate output from the still is collected in a bottle to prevent yield re-evaporation of condensate. The amount of condensate was measured using a graduated jar cylinder and measured during the working day every 60 minutes time intervals.

Fig. 4. Photograph of the instruments in the experiment setup; a) the data acquisition and k-type thermocouples, b) the conductivity / TDS device, c) the solar power meter, d) wind speed meter.

C. Solar Still Daily Thermal Efficiency

The daily thermal efficiency of the solar still, η_d, was evaluated according to the hourly production m, the latent heat of vaporization h_{fg}, the daily average solar radiation $I(t)$ and the water area A_w of the device as reported by Velmuruga *et al.* [23] as (1).

$$\eta_d = \sum \dot{m} \times h_{fg} / \sum A_w \times I(t) \quad (1)$$

The percentage increase in daily thermal efficiency of enhanced solar still compared with the conventional solar still at 3 cm water depth.

D. Experimental Uncertainty Analysis

In this work, Holman [24] method is used to estimate the uncertainty in experimental results. The minimum calculated error is expressed as the ratio between the device's least count and the measured minimum value of the output [25]. The uncertainties of the different parameters of the experimental work are shown Table II.

TABLE II: UNCERTAINTIES IN THE DIFFERENT PARAMETERS

Instrument	Uncertainty
Solar power meter	±0.050%
K-type thermocouples	±0.060%
Water productivity	±0.125%
The wind velocity	±0.56%
Water conductivity	±0.0001%
Water TDS	±0.0002%

E. The Experimental Procedure

Experiments were performed at faculty of Engineering, University of Tabuk and carried out from 7 A.M to 7 P.M. The experimental work was performed for four months (From May to August 2021). The absorber, water, space and glass temperatures inside the still, water productivity, solar radiation, and wind velocity were measured every 60 minutes time intervals. The accumulated water productivity is also measured in each experiment at the working day end. Ambient temperature was measured as the daily weather characteristics. Water conductivity and TDS were measured at the beginning and end of each experiment.

III. SOLAR RADIATION MODELING

Sakonidou *et al.* [26] used Duffie and Beckman relations [27] to calculate the hourly solar radiation components. The total daily irradiation on a horizontal plane, H, is expressed as a function of beam (H_b) and diffused (H_d) irradiation, shown in (2).

$$H = H_b + H_d \quad (2)$$

The daily extraterrestrial solar irradiation, H_o on a horizontal plane is given [26] as (3).

$$H_o = \frac{24 \times 3600}{\pi} S_c \left(1 + 0.033 \cos \frac{360N}{365}\right) \times \left[\cos\phi \cos\delta \sin\omega_s + \frac{\pi \omega_s}{180} \sin\phi \sin\delta\right] \quad (3)$$

where S_c is constant, N is the day of the year and ω_s is the sunset hour angle given as (4) and (5).

$$\omega_s = \arccos(-\tan\phi \tan\delta) \quad (4)$$

ϕ and δ are latitude and declination angles respectively.

The clearness index, $k_T = H / H_o$ (5)

The diffuse component, H_d can be calculated based on the values of the clearness index as shown in (6) and (7). For $\omega_s \leq 81.4°$,

$$\frac{H_d}{H} = \begin{cases} 1.0 - 0.2727k_T + 2.4495k_T^2 - 11.9514k_T^3 \\ + 9.3879k_T^4 \quad for \quad k_T < 0.715 \\ 0.143 \quad for \quad k_T \geq 0.715 \end{cases} \tag{6}$$

For $\omega_s > 81.4°$

$$\frac{H_d}{H} = \begin{cases} 1.0 + 0.2832k_T - 2.555k_T^2 \\ + 0.8448k_T^3 \quad for \quad k_T < 0.722 \\ 0.143 \quad for \quad k_T \geq 0.722 \end{cases} \tag{7}$$

The ratio of the total hourly irradiation, I_t, over the total daily irradiation, H, is given by (8)

$$r_t = I_t / H \tag{8}$$

and can be calculated with (9).

$$r_t = \frac{\pi}{24}\left(\alpha + \beta_c \cos\omega\right)\frac{\cos\omega - \cos\omega_s}{\sin\omega_s - \frac{\pi\omega_s}{180}\cos\omega_s} \tag{9}$$

where the coefficients α and βc are given in (10) and (11).

$$\alpha = 0.409 + 0.5016\sin(\omega_s - 60) \tag{10}$$

$$\beta_c = 0.6609 - 0.4767\sin(\omega_s - 60) \tag{11}$$

The ratio of the hourly diffuse irradiation, Id over the daily diffuse irradiation, H_d, is given in (12).

$$r_d = I_d / H_d \tag{12}$$

Substituting into equations, this value can be rewritten as (13).

$$r_d = \frac{\pi}{24}\frac{\cos\omega - \cos\omega_s}{\sin\omega_s - \frac{\pi\omega_s}{180}\cos\omega_s} \tag{13}$$

Then, I_t and I_d are calculated from equations, whereas the hourly direct irradiation, I_b, is computed as (14).

$$I_b = I_t - I_d \tag{14}$$

The total radiation on a tilted surface of β, is given by (15).

$$I = I_b R_b + I_d\left(\frac{1+\cos\beta}{2}\right) + I_t\, r_g\left(\frac{1-\cos\beta}{2}\right) \tag{15}$$

where r_g is the diffuse reflectance of the surroundings (equals to 0.25).

IV. Mathematical Modeling of Solar Still Productivity

The hourly output per m^2 from the solar still can be obtained [28] using (16).

$$m_{ew} = q_{ew}\, A\, t / h_{fg} \tag{16}$$

Where, t is the time, $q_{ew} = h_{ew}(T_w - T_g)$ and $h_{ew} = 0.01623h_{cw}(P_w - P_g)/(T_w - T_g)$, and the latent heat of vaporization is $h_{fg} = \left(2503.3 - 2.398T_w\right) \times 1000$

$$P_g = \exp\left[25.317 - \frac{5144}{T_g + 273}\right] \tag{17}$$

$$P_w = \exp\left[25.317 - \frac{5144}{T_w + 273}\right] \tag{18}$$

Dunkle [29] presented a convective heat transfer correlation in (19).

$$h_{cw} = 0.884\left(\Delta T\right)^{1/3} \tag{19}$$

where $\Delta T = \left[(T_w - T_g) + \frac{(P_w - P_g)(T_w + 273.15)}{268.9 \times 10^3 - P_w}\right]$

Fig. 5 presents the flowchart of the main computer program for the modeling of solar radiation and solar still productivity.

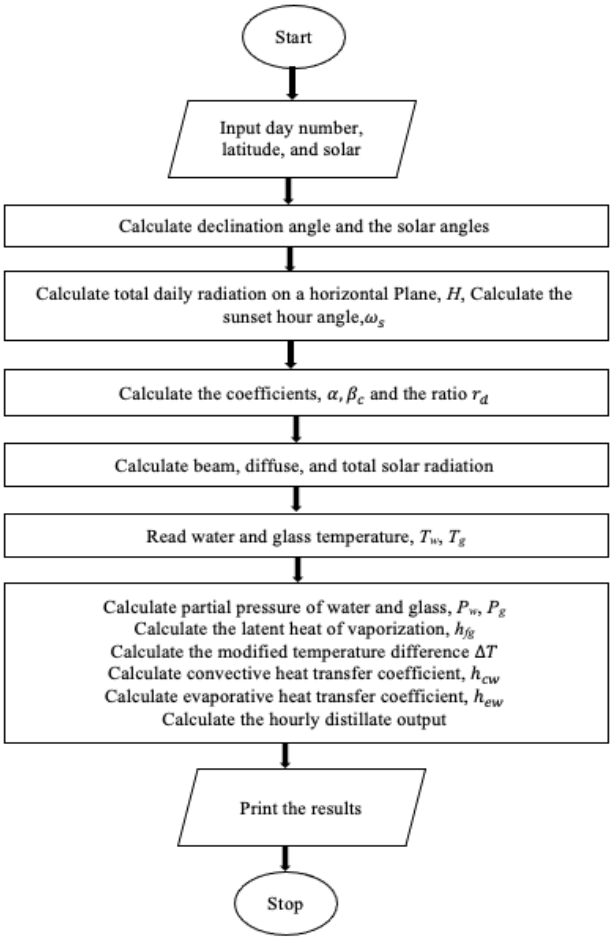

Fig. 5. Flowchart of the main computer program.

V. Statistical Evaluation Methods

In this study different statistical methods were used to compare the experimental and calculated results.

A. Coefficient of Determination (R^2)

The coefficient of determination R^2, can be used to evaluate the linear relation between calculated and measured values; this value should be closer to unity as possible and is given by (20) [29].

$$R^2 = 1 - \frac{\Sigma (I_{T,m} - I_{T,c})^2}{\Sigma (I_{T,m} - \bar{I}_{T,m})^2} \quad (20)$$

The term $\bar{I}_{T,m}$ in the equation is defined as (21) [30].

$$\bar{I}_{T,m} = \sum_{i=1}^{n_p} I_{T,m} / n_p \quad (21)$$

where, n_p is the number of experimental points.

B. Root Mean Square Error (RMSE)

The *RMSE*, provides data and information on the short-term performance of the used correlations. The minimum value of the *RMSE*; this means the best performance for the described model ('zero' is the ideal case). The *RMSE* is defined as (22) [31].

$$RMSE = \left(\frac{1}{n_p} \Sigma_{i=1}^{N} (I_{T,m} - I_{T,c})^2 \right)^{0.5} \quad (22)$$

C. Cost Evaluation of The Solar Still

Omara *et al.* [32] studied the cost comparison of different solar stills based on different factors such as the capital recovery factor, the fixed annual cost, the sinking fund factor, the annual salvage value, average annual productivity and annual cost. The calculation parameters can be expressed as (23), (24), (25), (26), (27), (28), (29) and (30).

$$CRF = i(1+i)^Z / [(1+i)^Z - 1] \quad (23)$$

$$FAC = PCC \left(CRF \right) \quad (24)$$

$$SFF = i / [(1+i)^Z - 1] \quad (25)$$

$$S = 0.2 \ (PCC) \quad (26)$$

$$ASV = \left(SFF \right) S \quad (27)$$

$$AMC = 0.15 \ FAC \quad (28)$$

$$AC = FAC + AMC - ASV \quad (29)$$

$$CPL = AC / AAP \quad (30)$$

where, S is constant, PCC is present capital cost of system, i is the interest which is assumed as 12% and z is the number of life years and assumed as 10 years.

VI. Results and Discussions

This section presents the results of solar radiation modeling, solar still performance, cost evaluation of the enhanced solar still, and the comparison between the measured and modeled results.

A. Weather Characteristics

The experimental work was performed for four months (From May to August 2021) in a clear sky condition during the experimental days. The weather characteristics include important parameters such as the solar radiation, the ambient temperature, and the wind velocity. Fig. 6 shows the variations of wind velocity during the corresponding working days with daytime. This figure also shows the average wind velocity during these days. From Fig. 6 it can be noticed that the average wind velocity ranged from 2.3 m/s to 3.47 m/s. Fig. 7 presents the variations of the solar radiation and ambient temperature during some working days in different months with daytime. From Fig. 7, it can be seen that, the global solar radiation increases from sunrise, reaches the maximum value at noon time and decrease again to sunset. The maximum recorded values of the global solar radiation for 7-6, 15-6, 22-6 and 20-7-2021 are 1050, 1070, 1100 and 1105 W/m^2 respectively.

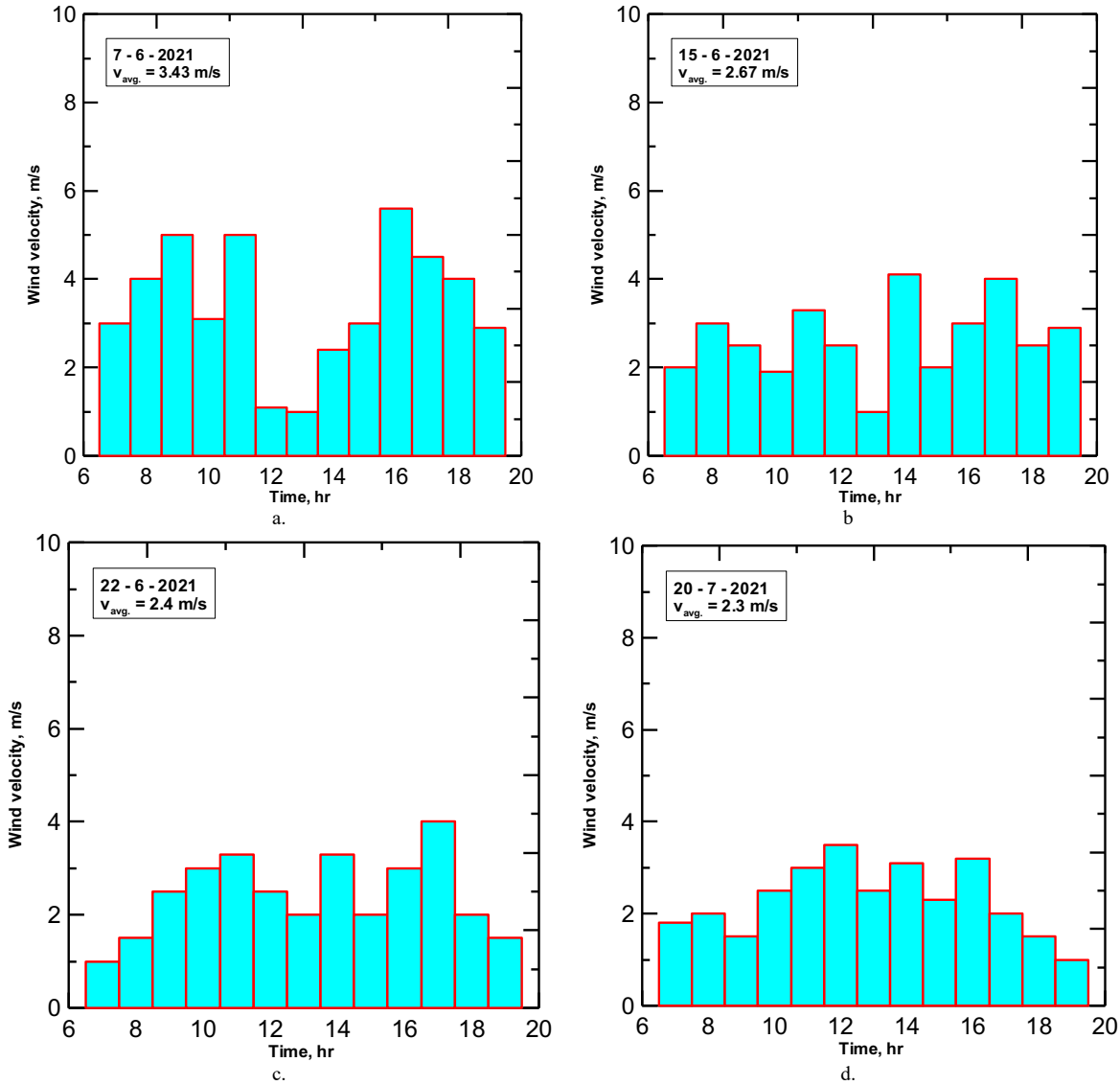

Fig. 6. The variations of wind velocity during the working days showing the average velocity; a) 7-6-2021, b) 15-6-2021, c) 22-6-2021, d) 20-7-2021.

B. Theoretical Results of Solar Radiation

Fig. 8 represents a comparison between the mathematical model and the measured data for the same working days at faculty of Engineering, University of Tabuk. From Fig. 8 it can be noticed that there is a small deviation between the predicted and measured values and any deviation occurred due to the unstable weather conditions during these months. Table III summarizes the statistical test results for the model during the working days. From Table III it is clear that the proposed mathematical model gives good prediction of solar radiation over all these months. It can be noticed that the coefficient of determination for 7-6, 15-6, 22-6 and 20-7-2021 are 0.98, 0.985, 0.975 and 0.98 respectively and the corresponding values for the root mean square error are 44.46, 37.45, 49.15 and 44.45 respectively. The obtained results from the mathematical modelling were evaluated and compared based on the measured results as reported by Ramzy *et al.* [33].

TABLE III: THE STATISTICAL ERRORS OF SOLAR RADIATION FOR MEASURED AND CALCULATED VALUES

Date	7-6-2021	15-6-2021	22-6-2021	20-7-2021
RMSE	44.46	37.45	49.15	44.45
R^2	0.98	0.985	0.975	0.98

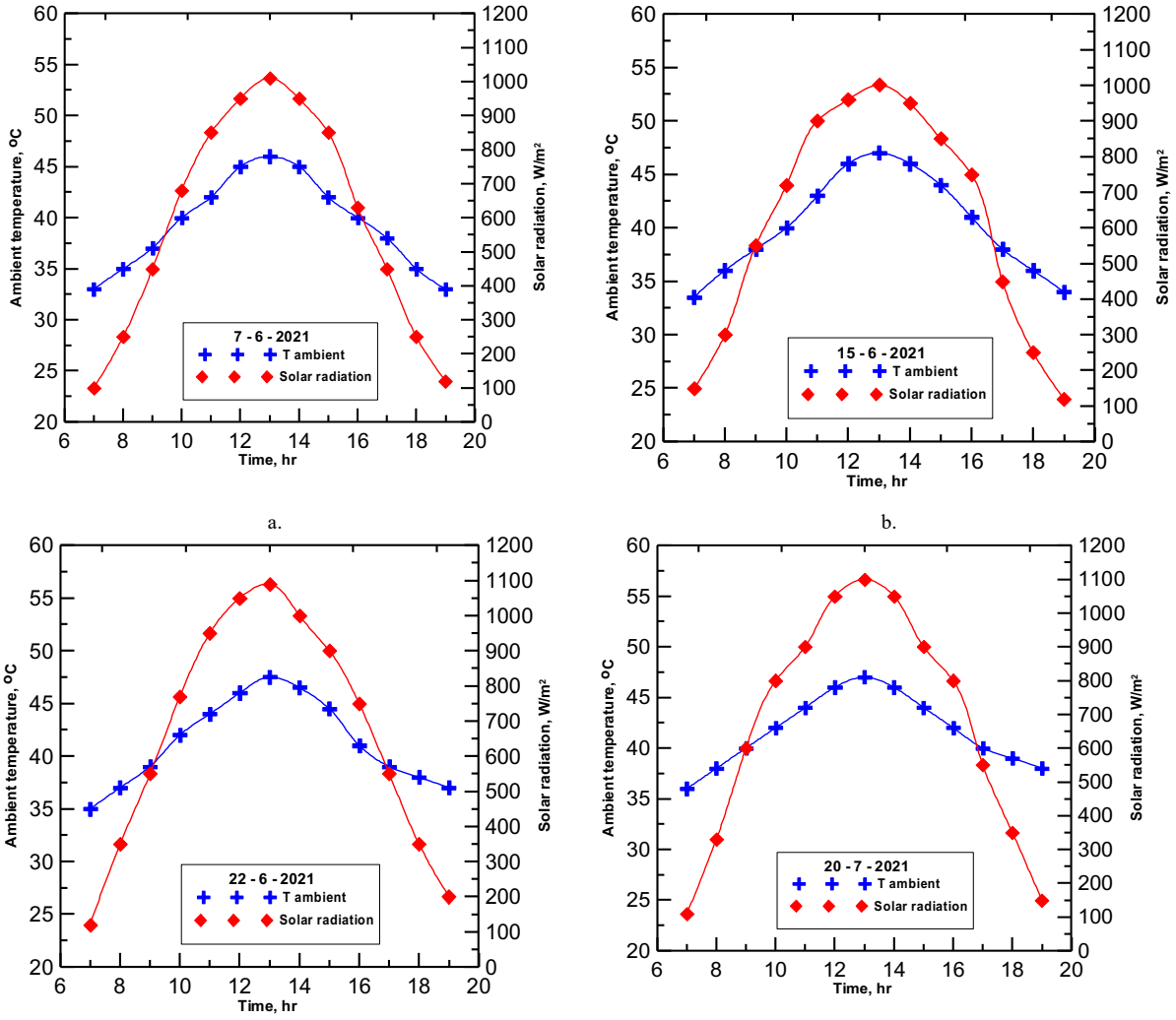

Fig. 7. The variations of ambient temperature and solar radiation during the working days; a) 7-6-2021, b) 15-6-2021, c) 22-6-2021, d) 20-7-2021.

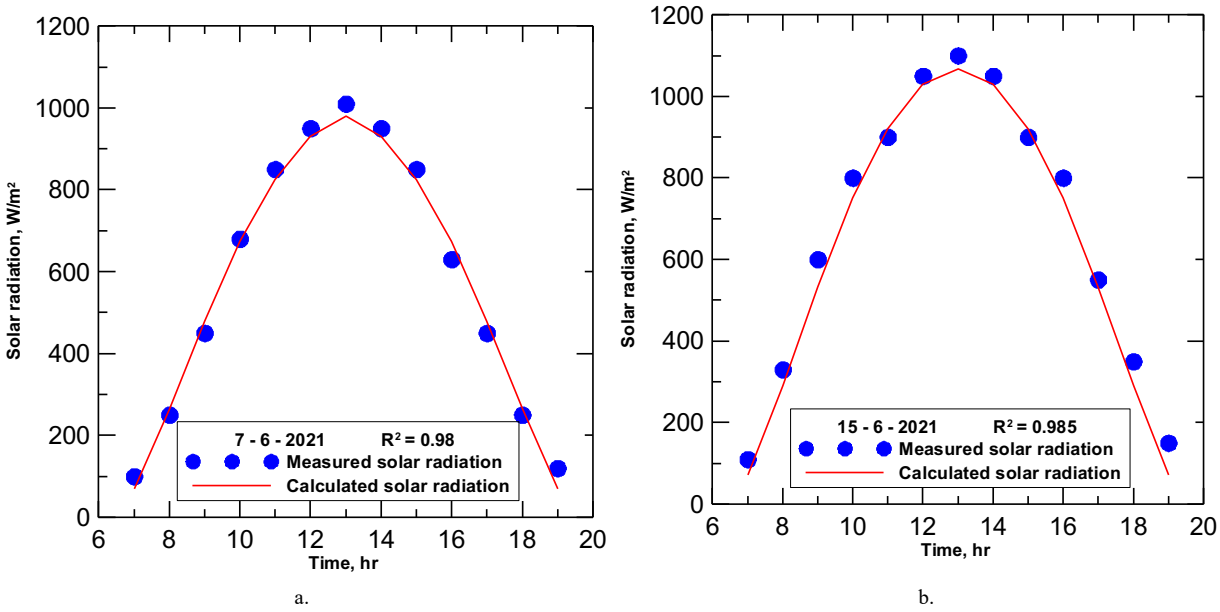

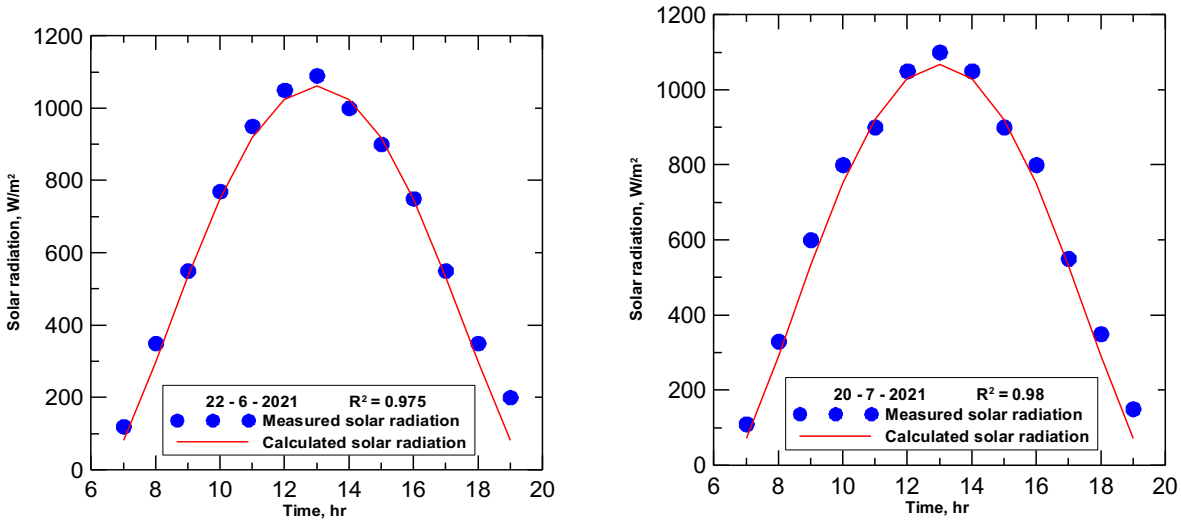

c. d.

Fig. 8. The hourly variations of measured and calculated solar radiation during the working days; a) 7-6-2021, b) 15-6-2021, c) 22-6-2021, d) 20-7-2021.

C. The Enhanced Solar Still Performance

Four similar clear days in climate conditions are chosen to compare results at a water depth of 3 cm for enhanced and conventional solar stills. Fig. 9 shows the temperature variation for the basin, water, space, and glass for enhanced and conventional solar stills. For the enhanced double slope glass solar still, at water depths of 3 cm, the absorber basin temperature reached a maximum value of 84.1°C. Also, the maximum water temperature value was 80.1°C. Each of space and glass temperatures is the average of two measured values, so the maximum average temperature values were 70.0 and 66.1°C respectively as shown in Fig. 9a. Finally for glass temperature, the maximum average recorded value was about 62.1°C respectively. It's very clear from this figure that, the absorber receives and absorbs the energy coming from the sun. The water production is collected within the waterway to measure the volume in the calibrated flask. All measured temperature distribution increased and reached its maximum value at about 13 o'clock, and then it began to decrease again. The conventional solar still shows a similar performance to the enhanced double slope glass solar still but the absorber, water, space and glass temperatures is lower than that of the enhanced one. For a water depth of 3 cm the maximum values for absorber, water, space and glass temperatures were 70.1, 67, 60.1 and 53.0°C respectively as shown in Fig. 9b. The high energy stored in the enhanced still causing an increase in absorber and water temperatures and increasing the productivity.

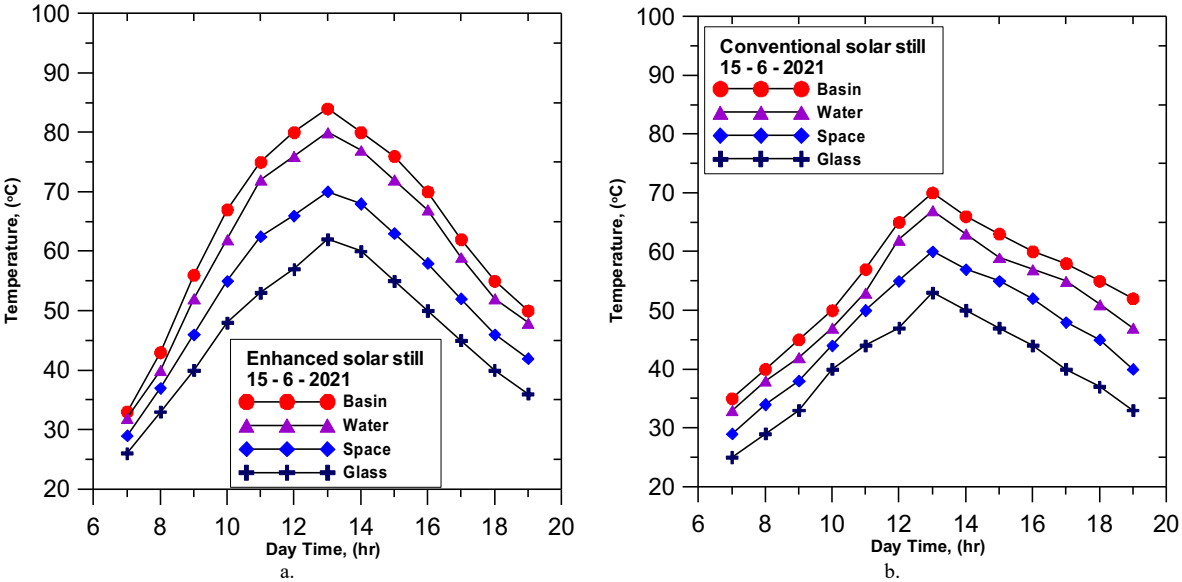

a. b.

Fig. 9. The hourly variations of basin, water, space and glass temperatures for conventional solar still during 15-6-2021; a) enhanced solar still, b) conventional solar still.

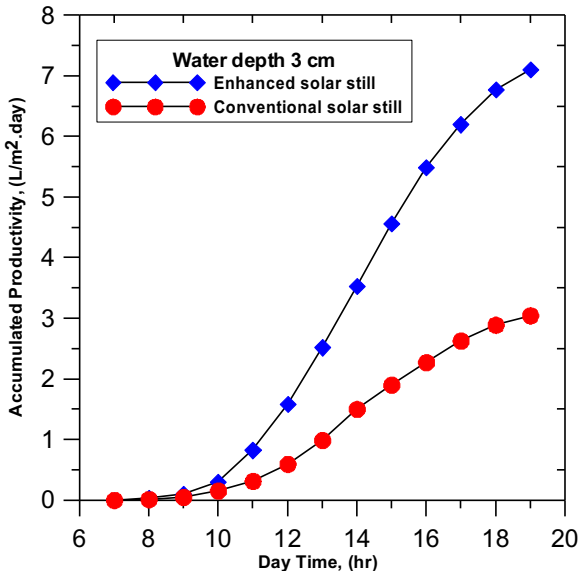

Fig. 10. The variations of accumulated productivity for enhanced and conventional still during 15-6-2021 at water depth of 3 cm.

Fig. 10 shows the hourly variations of accumulated productivity for enhanced and conventional solar still during 15-6-2021 at a water depth of 3 cm. From Fig. 10, it is clear that accumulated productivity for enhanced and conventional solar still was 7.104 and 3.046 respectively. The percentage of increase in accumulated productivity for enhanced solar still was about 57.12% compared with the conventional one.

D. Water Quality

The water quality of fresh and salty water before and after the desalination process is shown in Table IV. From Table IV it can conclude that the yield has the same values of total dissolved solids and conductivity approximately. The total dissolved solid is decreased from 30300 to 97.2 ppm, so solar desalination is one of the many processes used in purifying water for domestic use. At the end of the working day, two samples of salty water were taken and analyzed from the basin water in the solar still.

TABLE IV: QUALITY OF WATER

Water type	TDS (ppm)		Conductivity (µS/ cm)	
	Before	After	Before	After
Fresh	249	92.4	482	195.5
Salty	30300	97.2	40700	196.0

E. Comparisons Between Theoretical and Experimental Results for Enhanced Solar Still

Fig. 11 shows the comparison between calculated and experimental accumulated productivity for enhanced and conventional solar stills at a water depth of 3 cm for 15-6-2021. It is clear from the figure that, there is an acceptable agreement between the theoretical and experimental results for the enhanced and conventional one. The corresponding values for the determination coefficient were about 0.968 and 0.965 respectively. The measured, calculated accumulated production and daily efficiency for enhanced and conventional solar still at a water depth of 3 cm are shown in Table V. From Table V, it can be noticed that the maximum measured daily thermal efficiency was about 56.4% and 25.31% for enhanced and conventional solar still respectively. The corresponding values for the calculated thermal efficiency was about 59.8% and 29.2% respectively.

It is clear that the deviation of daily thermal efficiency of the enhanced and conventional one was small, and this indicates that, the proposed model gives good prediction for the still's performance. During the working days the average measured and calculated values of accumulated productivity for conventional solar still were 3.01 and 3.32 L/m^2.day respectively with a deviation of 9.3%. The corresponding average values for the enhanced solar still were 7.03 and 8.16 L/m^2.day respectively with a deviation of 13.8%. In other words, this is meaning that, using copper T shape pieces for solar still is considered the best solution to obtain potable water with more productivity and high value of daily thermal efficiency.

F. Cost Evaluation of The Enhanced Solar Still

The total cost of the enhanced solar still is about 302 $. Daily productivity is assumed to be 7.03 L/m^2 per day at a water depth of 3 cm, and still operates 340 days in a year, with a still life of 10 years. The total productivity is 23902 L. The cost of one liter from the enhanced solar still = 302/23902 = 0.013 $ (according to the prices in the year 2021).

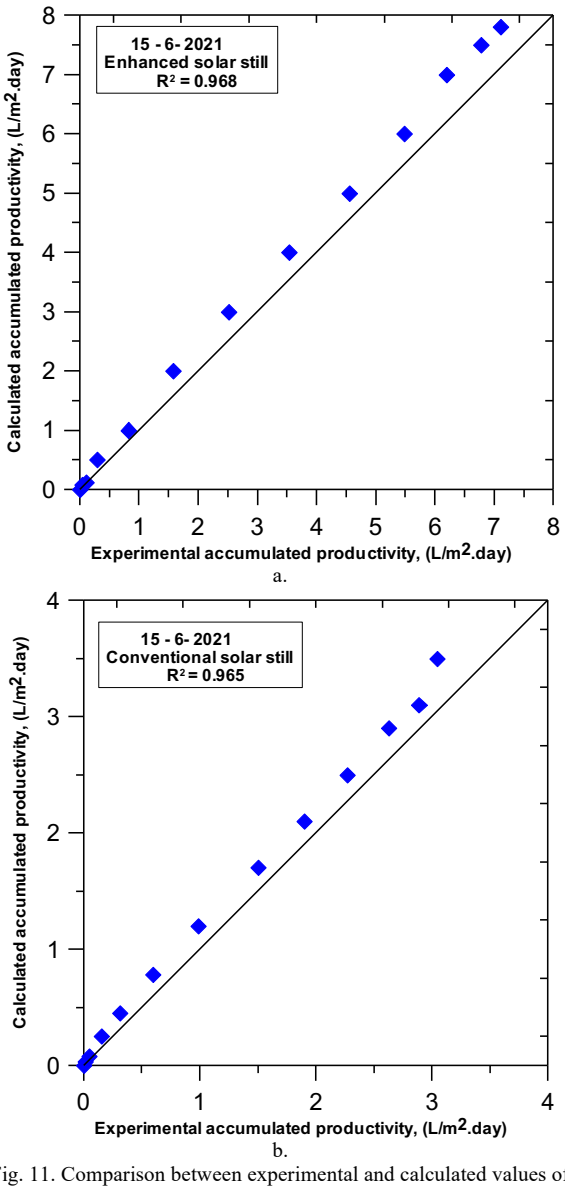

Fig. 11. Comparison between experimental and calculated values of accumulated production for enhanced and conventional one; a) enhanced solar still, b) conventional solar still.

TABLE V: MEASURED / CALCULATED ACCUMULATED PRODUCTIVITY AND DAILY EFFICIENCY FOR ENHANCED AND CONVENTIONAL ONE AT 3 CM WATER DEPTH

Date	Device	Measured values		Calculated values	
		Accumulated productivity L/m^2.day	Daily efficiency, η_d, (%)	Accumulated productivity L/m^2.day	Daily efficiency, η_d, (%)
7-6-2021	Conventional	3.04	25.31	3.32	27.2
	Enhanced	7.12	55.35	7.92	58.5
15-6-2021	Conventional	2.98	22.23	3.25	26.8
	Enhanced	6.85	52.52	7.85	57.2
22-6-2021	Conventional	3.13	26.10	3.31	27.1
	Enhanced	7.34	56.40	9.11	59.8
20-7-2021	Conventional	2.88	21.51	3.4	29.2
	Enhanced	6.79	50.34	7.75	56.8
Average	Conventional	3.01	23.79	3.32	27.58
	Enhanced	7.03	53.65	8.16	58.08

TABLE VI: COST EVALUATION FOR THE COMPONENTS OF THE ENHANCED AND CONVENTIONAL SOLAR STILLS ACCORDING TO THE YEAR 2021

Component	Enhanced solar still cost, ($)	Conventional solar still cost, ($)
Galvanized iron sheets	30	25
Glass cover	140	90
Support legs and wood sheets	30	25
Coating and primers	20	15
Rubber sheet and insulations	20	15
Clamps	12	10
Pipes, valves and fittings	20	20
copper T shape pieces	30	0
Total cost	302	200

TABLE VII: THE COST COMPARISON BETWEEN THE ENHANCED AND CONVENTIONAL SOLAR STILLS

Still type	*PCC* $	*AAP* L/m^2	*FAC*	*S*	*ASV*	*AMC*	*AC*	*CPL* $/L/m^2
Enhanced solar still	302	23902	53.45	60.4	3.443	8.02	58.03	0.0024
Conventional	200	10234	35.40	40.0	2.28	5.31	38.43	0.0037

In general, the cost of enhanced solar still was approximately 302 $ which is higher than that of any conventional types. Cost estimation for various components used in the in-house fabrication of the enhanced solar still is given in Table VI.

Table VII shows the cost comparison between enhanced and the conventional one. From this table it's clear that the enhanced solar still gives the highest accumulated productivity and the minimum values of the CPL.

VII. CONCLUSIONS

Fresh water is very important for human life, industrial production and biological health. Solar desalination technology is considered as one of the best solutions to obtain fresh water with low cost. This study presents a mathematical modelling and experimental evaluation for an enhanced double-slope glass solar still. Two similar solar stills were designed and fabricated at faculty of Engineering, University of Tabuk from May to August 2021. In addition water quality was measured before and after the experiments. Copper T shape pieces are used in the still basin to increase the still productivity at water depth of 3 cm. All measured and modelling results were evaluated based on the statistical evaluation methods such as (R^2) and (*RMSE*). The results concluded that the average measured and calculated values of accumulated productivity for conventional solar still were 3.01 and 3.32 L/m^2.day respectively with a deviation of 9.3%. The corresponding average values for the enhanced solar still were 7.03 and 8.16 L/m^2.day respectively with a deviation of 13.8%. In addition it can be noticed that the maximum measured daily thermal efficiency was about 56.4% and 25.31% for enhanced and conventional solar still respectively.

REFERENCES

[1] Brika B. Water Resources and Desalination in Libya: A Review. Proceedings. 2018; 2(11):586. https://doi.org/10.3390/proceedings2110586.

[2] Kalogirou, S. Seawater desalination using renewable energy sources, *Progress in Energy and Combustion Science*, 2005; 31: 242-281. https://doi.org/10.1016/j.pecs.2005.03.001.

[3] Delyannis, E. Historic background of desalination and renewable energies, *Solar Energy*, 2003; 75(5):357-66. https://doi.org/10.1016/j.solener.2003.08.002.

[4] El-Agouz, SA. Experimental investigation of stepped solar still with continuous water circulation, *Energy Conversion and Management,* 2014; 86: 186-193. https://doi.org/10.1016/j.enconman.2014.05.021

[5] Elango T and Murugavel, KK. The effect of the water depth on the productivity for single and double basin double slope glass solar stills, *Desalination*, 2015; 359: 82-91. https://doi.org/10.1016/j.desal.2014.12.036.

[6] Kabeel A, Mohamed A, Mahgoub M. The performance of a modified solar still using hot air injection and PCM, *Desalination*, 2016; 379: 102–107. https://doi.org/10.1016/j.desal.2015.11.007.

[7] Ibrahem A, Saleh R, Mohammad B, Leema A, Sultan A, Muafag T, Experimental and numerical performance analysis and optimization of single slope, double slope and pyramidal shaped solar stills, *Desalination*, 2017; 423: 124-134. https://doi.org/10.1016/j.desal.2017.09.023.

[8] Hansen R, and Murugavel K. Enhancement of integrated solar still using different new absorber configurations: an experimental approach, *Desalination*, 2017; 422: 59–67. https://doi.org/10.1016/j.desal.2017.08.015.

[9] Rahbar N, Asadi A, and Fotouhi-Bafghi E. Performance evaluation of two solar stills of different geometries: tubular versus triangular:

experimental study, numerical simulation, and second law analysis, *Desalination*; 2018; 443:44–55. https://doi.org/10.1016/j.desal.2018.05.015.
[10] Saeed N, Habibollah S, Mehdi B, Experimental and analytical investigations of productivity, energy and exergy efficiency of a single slope solar still enhanced with thermoelectric channel and nanofluid, *Renewable Energy*, 2019; 135: 729-744. https://doi.org/10.1016/j.renene.2018.12.059.
[11] Pankaj D, Aman S, Yash K, Aman SR, Dhananjay RM, Performance evaluation of single slope solar still augmented with sand-filled cotton bags, *Journal of Energy Storage,* 2019; 25: 100888. https://doi.org/10.1016/j.est.2019.100888.
[12] Gnanaraj SJ, Velmurugan V. An experimental study on the efficacy of modifications in enhancing the performance of single basin double slope solar still, *Desalination*, 2019; 467: 12-28, https://doi.org/10.1016/j.desal.2019.05.015.
[13] Kabeel A, Mohamed A. Enhancement of pyramid-shaped solar stills performance using a high thermal conductivity absorber plate and cooling the glass cover, *Renewable Energy*, 2020; 146: 769–775. https://doi.org/10.1016/j.renene.2019.07.020.
[14] Abdullah AS, Essa FA, Bacha HB, Omara ZM. Improving the trays solar still performance using reflectors and phase change material with nanoparticles, *Journal of Energy Storage,* 2020; 31: 101744. https://doi.org/10.1016/j.est.2020.101744.
[15] Kabeel AE, El-Maghlany WM, Abdelgaied M, Abdel-Aziz MM. Performance enhancement of pyramid-shaped solar stills using hollow circular fins and phase change materials, *Journal of Energy Storage*, 2020; 31: 101610. https://doi.org/10.1016/j.est.2020.101610.
[16] Sharshir SW, Ismail M, Kandeal AW, Faisal BB, Eldesoukey A and Younes MM. Improving thermal, economic, and environmental performance of solar still using floating coal, cotton fabric, and carbon black nanoparticles, *Sustainable Energy Technologies and Assessments*, 2021; 48: 101563. https://doi.org/10.1016/j.seta.2021.101563.
[17] Saravanan NM, Rajakumar S, Moshi AM. Experimental investigation on the performance enhancement of single basin double slope solar still using kanchey marbles as sensible heat storage materials, *Materials Today: Proceedings*, 2021; 39: 1600-1604. https://doi.org/10.1016/j.matpr.2020.05.710.
[18] Agrawal R. and Singh KD. Performance evaluation of double slope solar still augmented with binary eutectic phase change material and steel wool fibre, *Sustainable Energy Technologies and Assessments*, 2021; 48: 101597. https://doi.org/10.1016/j.seta.2021.101597.
[19] Parsa SM, Yazdani A, Dhahad H, Alawee WH., Hesabi S, Norozpour F, Davoud JY, *et al*. Effect of Ag, Au, TiO_2 metallic /metal oxide nanoparticles in double-slope solar stills via thermodynamic and environmental analysis, *Journal of Cleaner Production*, 2021;311: 127689. https://doi.org/10.1016/j.jclepro.2021.127689.
[20] Jobrane M, Kopmeier A, Kahn A, Cauchie H, Adel K, Christian P. Theoretical and experimental investigation on a novel design of wick type solar still for sustainable freshwater production, *Applied Thermal Engineering*, 2022; 200: 117648. https://doi.org/10.1016/j.applthermaleng.2021.117648.
[21] Abdelgaied M, Abdulla AS, Abdelaziz GM, Kabeel AE. Performance improvement of modified stepped solar distillers using three effective hybrid optimization modifications, Sustainable Energy Technologies and Assessments, 2022; 51: 101936. https://doi.org/10.1016/j.seta.2021.101936.
[22] Ahmed E, Ramzy K, Mansour TM, Ismail TM and Dawood MM. Solar Stills Performance and Productivity Enhancement Methods – A detailed Review, *American Journal of Engineering Research* (AJER), 2020; 9(01): 307-329.
[23] Velmurugan V, Deenadayalan CK, Vinod H, Srithar K. Desalination of effluent using fin type solar still, *Energy*, 2008; 33: 1719 - 1727. https://doi.org/10.1016/j.energy.2008.07.001.
[24] Holman, JP. Experimental Method for Engineers, 1994, 6th ed. McGraw-Hill, Singapore.
[25] Kabeel AE. Performance of solar still with a concave wick evaporation surface, *Energy*, 2009; 34: 1504-1509. https://doi.org/10.1016/j.energy.2009.06.050.
[26] Sakonidou EP, Karapantsios T D, Balouktsis AI and Chassapis D. Modeling of the optimum tilt of a solar chimney for maximum air flow, *Solar Energy*, 2008; 82: 80-94. https://doi.org/10.1016/j.solener.2007.03.001.
[27] Duffie JA, Beckman WA. Solar Engineering of Thermal Processes, second ed. Wiley-Interscience, New York, 1991, pp. 3-146.
[28] Kumar S and Tiwari GN. Estimation of convective mass transfer in solar distillation system, *Solar Energy*, 1996; 57: 459–64. https://doi.org/10.1016/S0038-092X(96)00122-3.
[29] Dunkle RV. Solar water distillation, the roof type solar still and a multi effect diffusion still, international developments in heat transfer, *ASME Proceedings of International Heat Transfer*, 1961; 5: 895-902.
[30] Maindonald J and Braun J. Data analysis and graphics using R- an example-based approach, second edition, 2006, published in the United States of America by Cambridge University Press, New York.
[31] Robaa, SM. Validation of the existing models for estimating global solar radiation over Egypt, *Energy Conversion and Management*; 2009; 50: 184-193. https://doi.org/10.1016/j.enconman.2008.07.005.
[32] Omara ZM, Kabeel AE, Younes MM. Enhancing the stepped solar still performance using internal and external reflectors, *Energy Conversion and Management*; 2014; 78: 876 - 881. https://doi.org/10.1016/j.enconman.2013.07.092.
[33] Ramzy K, Hussien AA, Shams El-Din, Gad HE and Elshamy MA. Simple New Developed Model for Forecasting the Solar Radiation in Egypt, *American Journal of Engineering Research* (AJER), 2020; 9(1):398-414.

Dr. Mohammed Alswat is currently working as an assistant Professor and chairman of Mechanical department, Faculty of Engineering, University of Tabouk, Saudi Arabia. He finished his Ph.D. from Northeastern University and published more than ten papers in international journals and conferences.